Mesomechanical Modeling of the Mechanical Behavior of Parachute Suspension Lines using LS-DYNA®

Catherine P. Barry[1], Francesco Panerai[2], Keith Bergeron[3],
Christine Charette[4], Gregory Noetscher[4], Scott E. Stapleton[1], David J. Willis[1],
James A. Sherwood[1]

[1]*University of Massachusetts Lowell*
[2]*University of Illinois at Urbana Champaign*
[3]*U.S. Army Corps of Engineers, Engineering Research and Development Center, Vicksburg, MS*
[4] *United States Army Combat Capabilities Development Command-Soldier Center, Natick, MA*

Abstract

Parachute suspension lines can develop vortex-induced vibrations while in flight, degrading the flight performance and creating noise. To understand the braid design factors associated with this vibration, the mechanical behavior of the braided parachute suspension line can be investigated using a fluid-structure interaction (FSI) analysis. Such an FSI analysis requires a well characterized macroscopic model of the axial, bending and torsional stiffnesses of the line. In the current study, a novel model using a combination of truss elements embedded in solid elements for capturing the asymmetric axial tension-compression stiffness of a tow as well as the lateral compression is presented. Tensile and transverse compression experiments were performed on the individual tows to characterize the axial and transverse stiffnesses to be used with the finite element model. Finite element models of the tow material characterization tests were compared with experimental data to calibrate the material model parameters and to validate the modeling approach. The mesoscale of a suspension line was resolved under zero load using X-ray computed tomography and data were used as the baseline image to generate a finite element model of a representative unit cell of the line. The Virtual Textile Morphology Suite (VTMS) and LS-PrePost® were used to obtain the geometry and mesh, respectively. The feasibility to use the novel modeling approach for capturing the mechanical behavior of the braid is demonstrated.

Introduction

Parachute suspension lines are used by the U.S. army to deliver supplies to personnel in the field [1]. When these parachutes are in flight, the suspension lines experience vibrations which create noise that can be heard for several kilometers. The vibrations of the lines also impede the ability of GPS-guided parachutes to land directly on target. It is believed that this vibration is a consequence of vortex-induced vibration. Vortex-induced vibration occurs when a bluff body is subjected to a cross-flow of air. The air touches the front boundary of the object and as the air approaches the back boundary of the object it separates resulting in the shedding of periodic air vortices. Vortex shedding induces fluctuating drag and lift forces on the object causing it to vibrate.

Recent studies on the vortex-induced vibration of parachute suspension lines have shown that a parachute suspension line has three distinct modes of vibration while in flight: a bending mode, a torsional mode, and a combination of the first two. Also, researchers found that the resulting frequency and amplitude were a function of the state of axial tension on the line and Reynolds number condition [2-9]. The findings from these studies revealed that the vibrational response of the line can be changed by controlling how the effective mechanical behavior of the line (bending stiffness and torsional stiffness) changes with axial tension.

Parachute suspension lines are made by braiding. The tows are initially braided in a circular pattern thereby creating a tube-like shape. The suspension line is then compressed between rollers and the circular shape becomes more of a rounded rectangular shape (Fig.1). The process results in a complex structure where the macroscopic mechanical behavior and the surface topology change as a function of the state of axial tension.

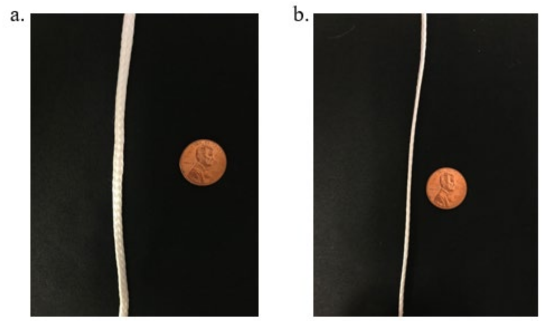

Figure 1: 16 tow suspension line:
(a.) side view and (b.) front view.

A suspension line is a textile structure, and textile structures have a hierarchal form. For the suspension line that is being evaluated on the smallest level, there are fibers and a group of fibers create a tow and some specified number of these tows are braided together to create a braided suspension line. Because of this hierarchy, the modeling of textile structures can have three different levels of approach: (1) macromechanical modeling (a macroscopic model of the braided line), (2) mesomechanical modeling (modeling to the level of the tows in the braided line) and (3) micromechanical modeling (modeling down to the level of the fibers comprising the tows). These different modeling levels are presented in Fig. 2. These three diffent levels of modeling (macro, meso, micro) all have advantages as well as disadvantages. When modeling a textile on the macro scale the controbutions of the fibers and the tows are condensed into a single solid part. Modeling this way eliminates the need for contact interactions of the tows and fibers making it computationally efficient, however, because the mechanical behavior is simplified into one part the detail of how the geometery changes with different loading conditions is not captured. The meso scale modeling approach models the textile down to the tow level. While this level of modeling is able to capture the tow-to-tow interaction and the change in geometery with a change in load the added complexity of the contact interaction between tows makes this type of modeling computationally intensive. Finally modeling at the micro scale captures the full detail of the textile structure with both fiber-to-fiber and tow-to-tow interactions. However this method is very computationaly intesive with all the contact that goes into this modeling. To compromise with geometery defininition and computational time the suspension line will be modeled at the meso-level.

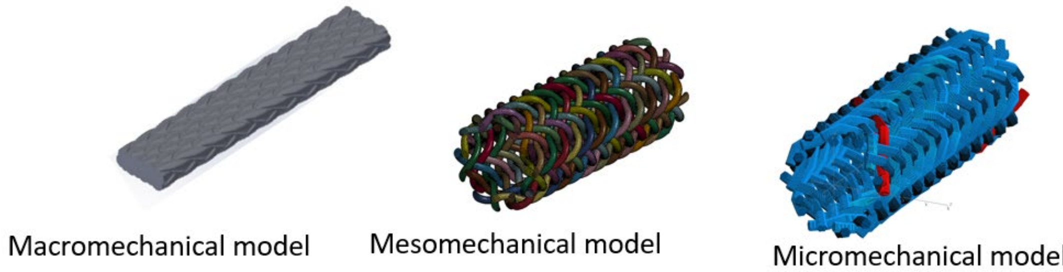

Figure 2: Levels of finite element modeling of textiles.

This paper presents the investigation of a mesomechanical finite element model of a braided 16-tow ultra high molecular weight polyethylene parachute suspension line. The mechanical properties for the finite element model of the tows that comprise the braid are found through an experimental characterization of individual tows. A novel approach of using solid elements with embedded trusses is used to model the orthotropic mechanical behavior and the asymmetric tension-compression axial stiffness of the tows. X-ray computed tomography (CT) data of the suspension line are used to get a baseline geometry for the braided line. The tows of this baseline braid are modeled using the proposed novel model. The credibility of the modeling approach is demonstrated for replicating the characterization tests of the individual tows and lateral compression and axial loadings of the braid.

Methods

Experimental and numerical methods were used to assist in the building of a finite element model of the parachute suspension line. Experimental methods were used to characterize the material properties of the individual tows of the suspension line, specifically the axial and transverse stiffnesses to be used in the finite element model. The suspension line itself was also characterized experimentally to be compared with the model for validation purposes. Numerical methods were used to create the finite element model of the parachute suspension line from CT-scan data and to simulate the experimental characterization tests.

Experimental Characterization

To explore if there was any difference in the effective stiffness as a function of material history, both "fresh off the spool", i.e. virgin, and previously in-braid tows were characterized. The axial elastic modulus was determined from the load-displacement response of pulling a tow in a Universal Testing Machine (Fig. 3). A gage length of 20 in. (0.51 m) was previously determined to be the optimal length for such testing [10]. The ends of the tows were super glued to square pieces of paper to increase the surface area in the pressurized clamps to mitigate slipping (Fig. 3). The crosshead speed that was used was 10 in/min (0.00423 m/s). The transverse compressive stiffness was determined through crush tests of bundles of fibers (Fig. 4). Groups of tows pulled from a virgin fiber roll and from a braid were grouped and tied to two 100-g weights. The weights kept the fibers together and comingled. A preload of 0.3 lbs (1.33 N) was put on the fiber bundle to maintain the initial gage length among the compression tests. The crosshead speed was set to 0.02 in/min.

Figure 3: Tensile test of a single tow.

Figure 4: Compression tests of tow bundles.

Transverse compression tests were also performed on the braided suspension line using the same experimental setup as was used with the testing of the tows. A braid was placed on the test fixture and a preload of 0.3 lbs (1.33 N) was applied. The crosshead speed was set to 0.02 in/min.

Modeling Methods

The braid that is being modeled consists of 16 tow bundles of ultra-high molecular weight polyethylene fibers. Modeling the structure down to the tow level will provide the ability to capture the contact interaction between the tows and how the surface geometry, bending and torsional stiffness change as a function of load condition.

Before a robust finite element model of the tow can be built, it is important that the model of the tows is able to capture the complex mechanical behavior of the tows. The tows exhibit anisotropic behavior where they have a very high axial tensile stiffness in comparison to their transverse compressive stiffness. The bending and compressive axial stiffnesses of an individual tow are very low (almost zero) in comparison to their axial tensile stiffness. Simple single tow models were created to see if it was possible to capture these differing behaviors as a function of the load direction, i.e. axial tension, lateral compression and axial compression. The axial compression evaluates the bending stiffness through the resulting buckling response.

A cylinder of solid elements was created in LS-PrePost to be representative of a single "straight" tow. To capture both the relatively high tensile stiffness in comparison to the low transverse compressive stiffness, "stiff" truss elements were embedded in "soft" solid elements. The trusses were chosen to incorporate the "high" axial tensile stiffness while the solid elements were chosen to incorporate the soft transverse compressive stiffness of the tows. The truss elements were made from the existing nodes that ran through the center of the cylinder made of solid elements (Fig. 5). The *MAT_ELASTIC (isotropic, linear elastic) material model was used for both the truss and the solid elements, the difference being the Young's modulus that was prescribed to each element type. The axial stiffness as determined from the experimental characterization tests of the tow was prescribed to the truss elements, and the transverse compressive stiffness obtained from experimental tests was assigned to the solid elements.

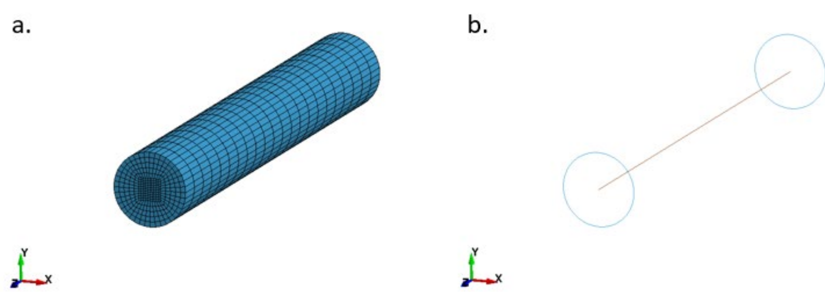

Figure 5: Finite element model of a single tow: (a.) Cylinder of solid elements and (b.) Truss elements running through the center of the cylinder.

When looking at the bending stiffness of an individual tow it can be seen without any experimental evaluation that the bending stiffness is extremely low. A single tow could be held in the air and even slight airflow over it results in a significant bend in the tow. This observation led to the conclusion that the bending stiffness should be treated as essentially zero in comparison to the axial stiffness. This essentially zero stiffness is accomplished through the combination of the low stiffness of the solid elements in combination with the "pin joints" connecting the chain of truss elements. To investigate that the model exhibited this very low bending stiffness, two Euler buckling conditions were studied with the cylinder model: pinned-pinned and clamped-clamped. The purpose was to see how much load it would take to get the model to buckle (low load would indicate low bending stiffness) and if it followed the Euler buckling theory (the clamped-clamped condition should be 4 times higher than the pinned-pinned condition). Boundary conditions were prescribed to the model and a displacement was prescribed at the "free" end (Fig. 6). The models were analyzed using LS-DYNA's implicit solver.

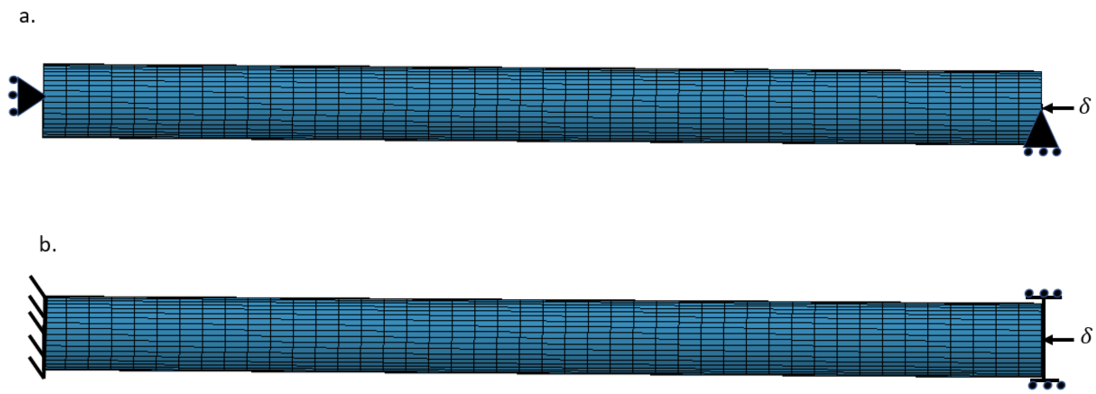

Figure 6: Buckling models of single tow: (a.) Pinned-pinned condition and (b.) Clamped-clamped condition.

To test if this method of modeling the tow was able to capture the axial stiffness, a tensile test was run on the cylinder. The cylinder was clamped on one end while a tensile displacement was prescribed to the other end using *BOUNDARY_PRESCRIBED_MOTION_SET.

To evaluate the compressive stiffness of the tow, a single tow was taken from the braid model that was created (creation of braid model described in next paragraph). The tow was taken from the braid model to incorporate the kinks and inconsistences of the initial state of the fiber bundles that were tested in compression. Four plates enclosed the tow so that it was free to move around but would not fly away as it was being crushed. Three of the plates were rigid except the top plate which was isotropic elastic. The top plate was isotropic elastic because it needed to be able to measure the reaction force from the tow during post-processing. The top plate had boundary conditions on it that would prevent the plate from deforming and that it could only move in the y-direction. All of the plates were fixed except the top plate that was prescribed a displacement in the negative y-direction. The back of the tow had rollers applied to it so it could not move in the x-direction. *CONTACT_SURFACE_TO_SURFACE was prescribed between the tow and the plates. Figure 7 illustrates this configuration.

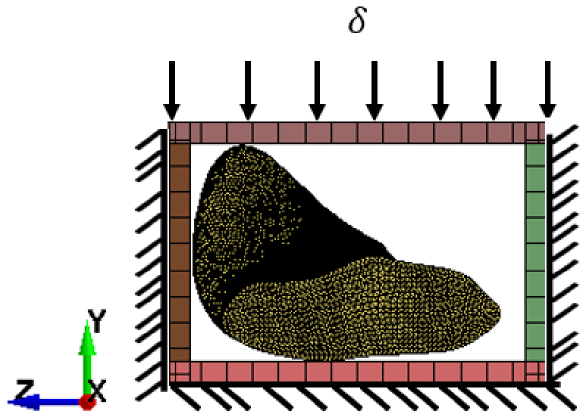

Figure 7: Compression of a single tow model.

The braid model was created using CT-scan data (Fig. 8) collected at the X-ray beamline 8.3.2 of Advanced Light Source at Lawrence Berkely National Laboratory. Imaging was performed at 25 ke V X-ray energy and 200 ms exposure, with the optical system described in [11], to achieve a spacial discretization 3.3 µm/pixel. The CT-Scan data of the braid under no load (0N) was used to define the initial geometry of the model. A Matlab code was used to perform image analysis on the CT-scan to identify and to assign coordinates to the individual fibers. The Matlab code is able to use these coordinates to write an input file for the Virtual Textile Morphology Suite (VTMS) software where the CT-scan data is then interpreted as a micro-scale model (Fig. 9). VTMS was developed at the Air Force Research Lab in Dayton, OH for the building of textile geometries on the micro, meso and macro scales. VTMS can take this model at the micro-scale and turn it into a meso-scale model (Fig. 10). This meso-scale model is a solid geometry that is meshed in the Gmsh and HyperMesh programs and imported into LS-PrePost for pre- and post-processing. The overall process is depicted in Figure 11.

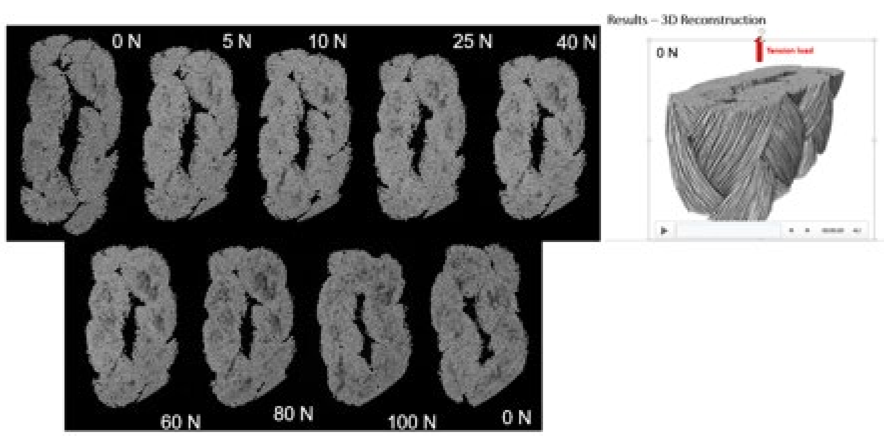

Figure 8: CT-scans of a parachute suspension line under various tensions.

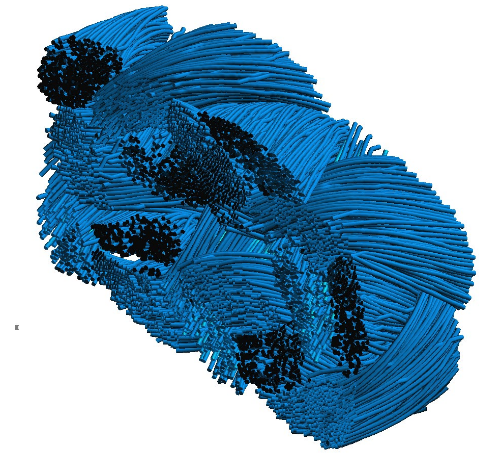

Figure 9: VTMS interpreted geometry of a suspension line from CT-scan data at no load.

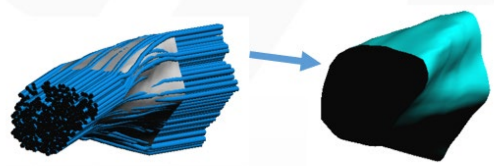

Figure 10: Tow meshing from a fiberized relaxed tow geometry.

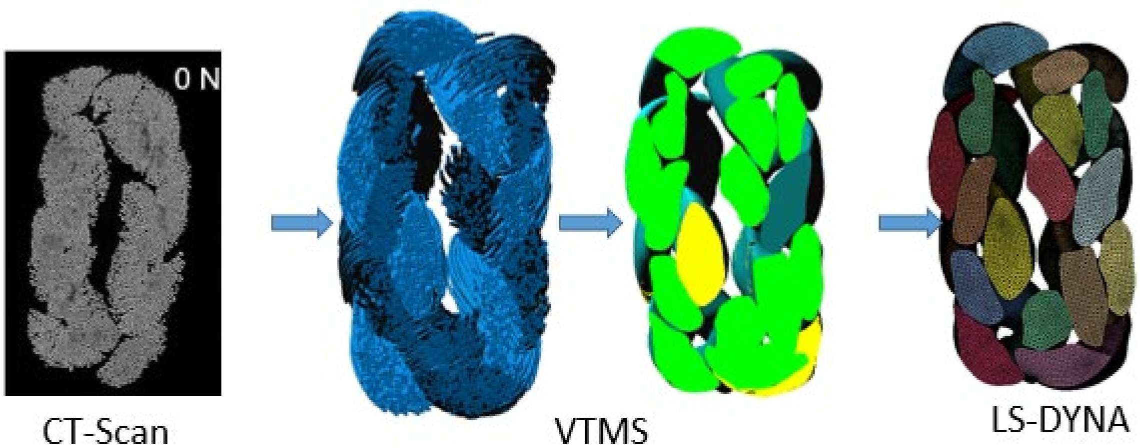

Figure 11: Overall process to obtain a mesoscale finite element model of the braid from CT-scan data.

Lastly the braid model was put through a transverse compressive test. Like the single tow setup version of this test, four plates enclosed the braid, and the top plate was prescribed a negative y-displacement. The back of the braid had rollers on it so it could not move in the z-direction. The *CONTACT_SURFACE_TO_SURFACE was prescribed among the 16 tows and the plates. The boundary conditions and model setup are presented in Figure 12.

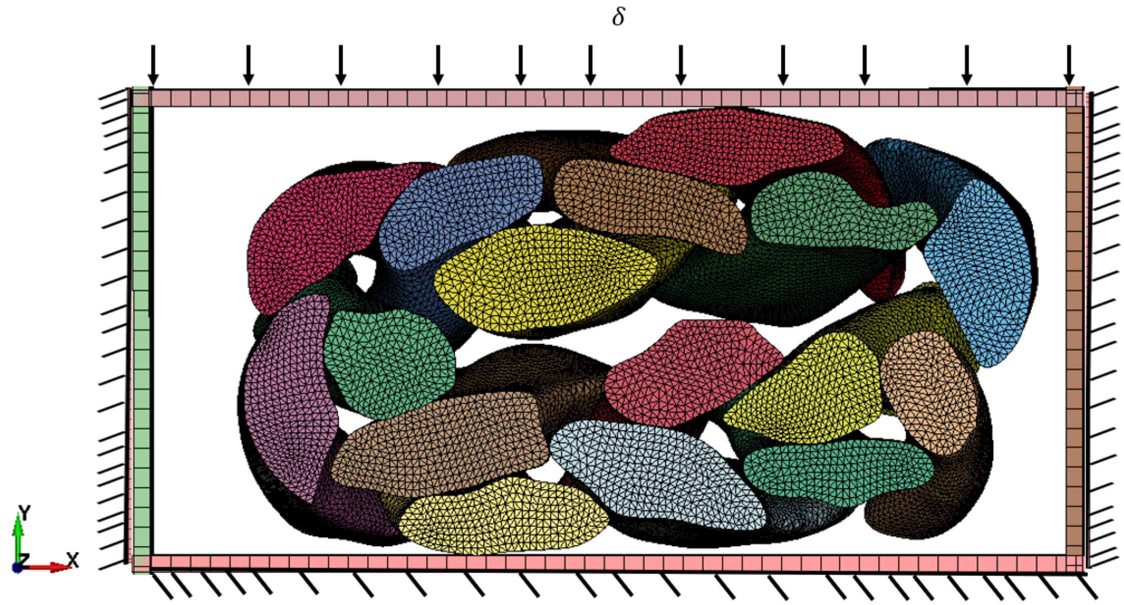

Figure 12: Compression test set-up of braid model

Results and Discussion

Tensile tests were preformed on a virgin fiber tow and a tow that was pulled out of a braid. Each test was run for five samples, and the results were averaged. Stress-strain curves were obtained, and the slope was calculated to obtain the axial modulus of a tow (Fig. 13). The modulus is around 78 GPa, and that was applied to the truss part of the tow model. The model was pulled in tension to repilcate the tensile tests, and stress-strain data was obtained (Fig. 13). As can be seen in Fig. 13, the model correlates well with experimental tensile tests. These results show that the model is able to represent the tow's axial stiffness.

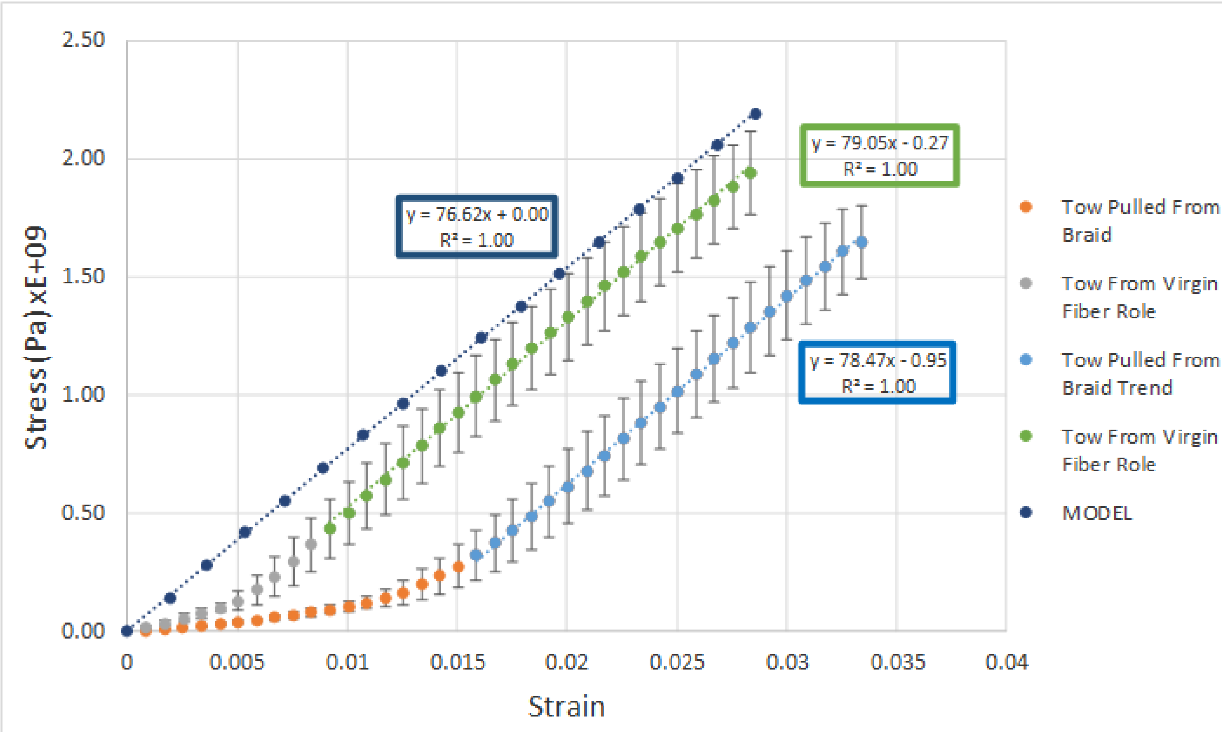

Figure 13: Stress-stain curves of experimental tensile tests compared with the tow model.

Compression tests were run on the tows to evaluate their transverse compressive stiffness. Tests were run on tows pulled from a spool of virgin fiber and a tows pulled from a braided suspension line. Stress-strain curves were obtained for both cases (Fig. 14). To get the elastic transverse compressive modulus from these curves, the linear ends of the curves were taken. The beginning parts of the curves are believed to be the part in the tests where the fibers are reorganizing and nesting into their final position where the transverse stiffness becomes linear and the elastic modulus can be calculated. The modulus that was obtained was about 1.93 MPa, and this value was applied to the solid elements of the tow model. The model of a single tow pulled from a braid was analyzed using LS-DYNA in compression and the stress-strain curve was obtained (Fig. 14). The graph shows that the model corelates well with the experimental data.

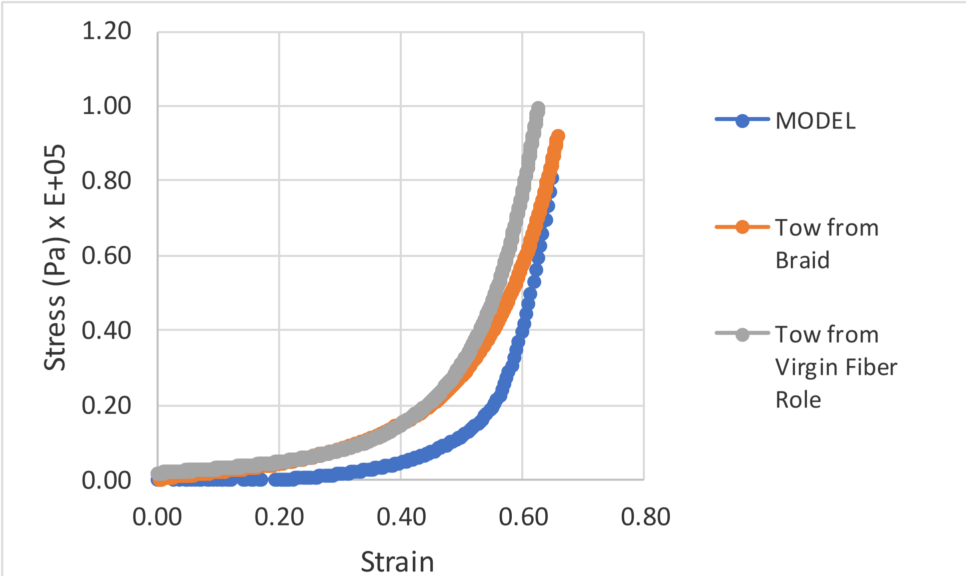

Figure 14: Stress-strain curves of compression tests of tows compared with tow model.

To evaluate the bending behavior of the model of a single tow, two Euler buckling conditions were investigated, i.e. pinned-pinned and clamped-clamped. The models were run in LS-DYNA implicit, and the resulting deformed shapes are given in Fig. 15. A graph of the load-displacement curves (Fig. 16) of the two models show that the load in both cases hits a peak and then drops when the structure buckles. From this graph, it can be concluded that the model follows the Euler buckling theory. The peak load, i.e. critical buckling load, for the pinned-pinned condition is 0.00281 N, and the peak load for the clamped-clamped condition is 0.00995 N which is about 4 times higher and is what Euler buckling theory states. These two models are also able show that modeling the tow this way can capture the very low bending behavior of the actual tow. The physical tow has a bending stiffness of almost zero, and the graph shows that the model has that low value as well because it takes very little load to get the model to buckle and significantly displace.

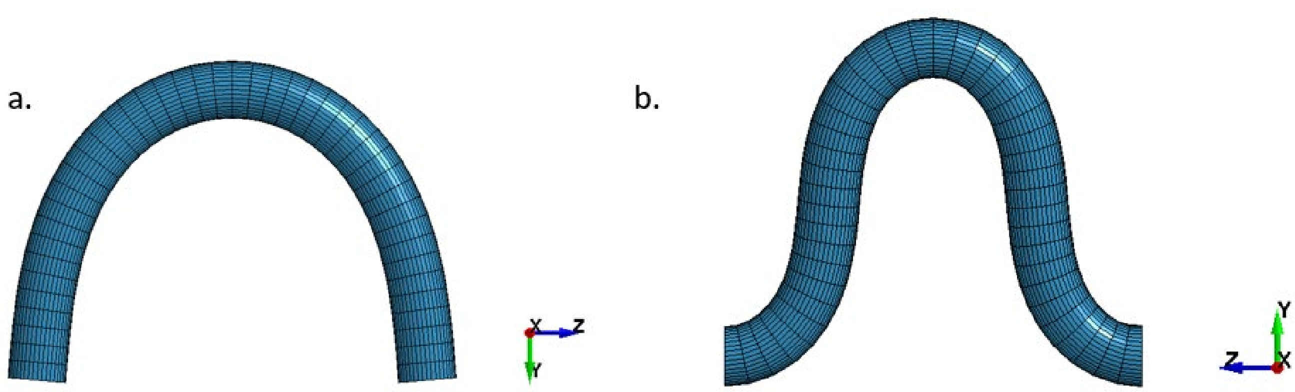

Figure 15: Deformation of tow buckling models (a.) Pinned-pinned (b.) Clamped-clamped.

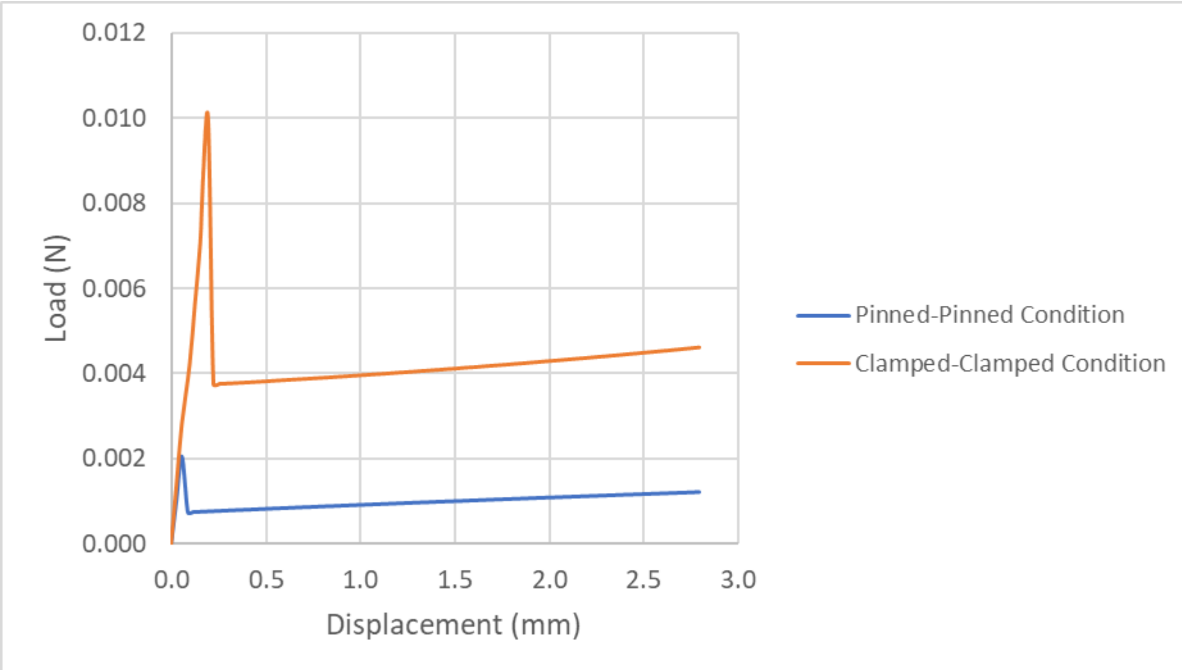

Figure 16: Load displacement curves of tow buckling models

The complete braid was compressed transversely to obtain experimental stress-strain data to be compared to the full braid model for validation purposes. Three compression tests of the braid were run to get the stress-strain data (Fig. 17). The braid model was run using the LS-DYNA implicit solver, and stress-strain data was analyzed (Fig. 17). The graph shows that the model of the braid can replicate the behavior of the full braid by using the axial and transverse elastic moduli as determined from the testing of the tows.

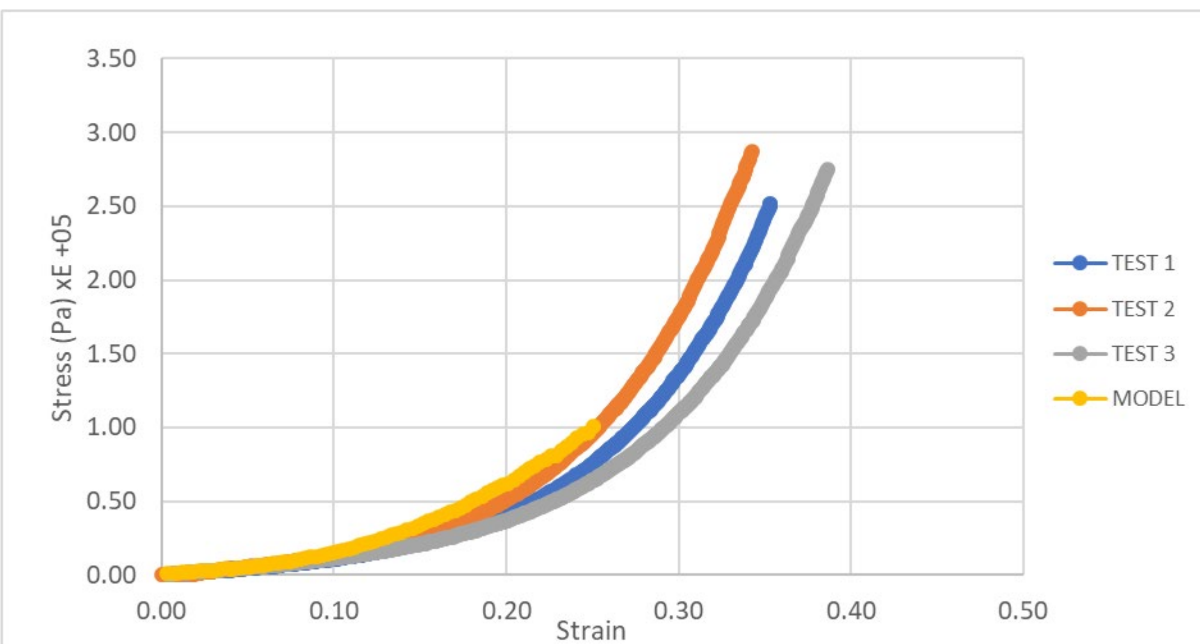

Figure 17: Stress-strain curves of the compression of the braid compared with the compression model of the braid.

The results show that the tows being modeled in this way are able to accurately depict the mechanical behavior of the physical tow under three different loading conditions. The full braid model made up of 16 of these tow models is also able to accurately capture the macroscopic transverse compression behavior of the physical braid.

Conclusions

This paper presented the investigation of a mesomechanical finite element model of a braided 16-tow ultra-high molecular weight polyethylene parachute suspension line. A novel approach of using solid elements with embedded trusses was used to model the orthotropic mechanical behavior and the asymmetric tension-compression axial stiffness of the tows. The mechanical properties of the tows were found through an experimental characterization of individual tows. Validation models that were run in LS-DYNA showed the ability of the truss elements embedded in the solid elements to correlate to the characterization tests and to predict the compressive load required to induce buckling. CT-scan data of the suspension line were used to get a baseline geometry for the braided line. The feasibility of using the mesomechanical model to capture the axial tensile and lateral compressive responses of the braid were explored.

Acknowledgements

The authors thank Patrick Drane and Kari White of UMass Lowell for their assistance and guidance of the experimental characterization of the tows. The authors also thank Matt Schey and George Barlow of UMass Lowell and Eric Zhou and David Mollenhauer of the Air Force Research Lab in Dayton, OH for their help and guidance with the use of the VTMS software. This research used resources of the Advanced Light Source, which is a DOE Office of Science User Facility under contract no. DE-AC02-05CH11231. The support of Drs. H. Barnard and D. Parkinson in collecting CT data is acknowledged. The authors acknowledge the U.S. Army Combat Capabilities Development Command, Soldier Center for its support of this work through Cooperative Agreement W911QY-15-2-0002.

References

1. Lingard S. Basic Analysis of Ram-Air Parachute. Precision Aerial Delivery Systems: Modeling, Dynamics, and Control. Progress in Astronautics and Aeronautics: American Institute of Aeronautics and Astronautics, Inc.; 2015. p. 73-125.
2. Siefers TM. Flow and Vibration Analysis of Parachute Suspension Lines. Colorado: University of Colorado at Colorado Springs; 2013.
3. Bergeron K, Curlett T, Ecklebe D, McClure K, Pitman B, Johari H, editors. Parachute Suspension Line Drag Analysis. 20th AIAA Aerodynamic Decelerator Systems Technology Conference and Seminar, Seattle, Washington; 2009.
4. Bergeron K, Daly S, Klausner A, Oliver M, Ranaweera R, editors. Streamwise and Spanwise Geometry Contributions to Parachute Line Drag. 21st AIAA Aerodynamic Decelerator Systems Technology Conference and Seminar.
5. Siefers T, McLaughlin TE, Bergeron K, editors. Wind Tunnel Characterization of Fluid-Structure Interactions for Various Suspension Lines. 44th AIAA Fluid Dynamics Conference, AIAA Aviation; 2014.
6. Siefers TM, Campbell JP, Clark DK, McLaughlin TE, Bergeron K, editors. Quantification of Drag from Flat Suspension Line for Parachutes and the Influence of Flow Induced Vibrations. 54th AIAA Aerospace Sciences Meeting, AIAA SciTech; 2016.

7. Siefers TM, Farrar WL, Jones CN, McLaughlin TE, Bergeron K, editors. Influence of Angle of Attack on Profile Drag and Flow Induced Vibrations of Parachute Suspension Lines. 24th AIAA Aerodynamic Decelerator Systems Technology Conference; 2017.
8. Siefers T, Greene K, McLaughlin T, Bergeron K. Wind and Water Tunnel Measurements of Parachute Suspension Line2013.
9. Pruett M, Accorsi M, Charles RD, editors. Validation of Computational Structural Dynamics Models for Parachute Systems. 20th AIAA Aerodynamic Decelerator Systems Technology Conference and Seminar, Seattle, WA, USA; 2009.
10. Barry C, Olson B, Bergeron K, Willis D, Sherwood J. Modeling Tensile Tests of a Braided Parachute Suspension Line using a Mesomechanical Finite Element Model2020.
11. MacDowell A, Parkinson D, Haboub A, Schaible E, Nasiatka J, Yee C, et al., editors. X-ray micro-tomography at the Advanced Light Source. Developments in X-Ray Tomography VIII; 2012: International Society for Optics and Photonics.